An $e^+e^-/\gamma\gamma/ep$ accelerator complex
at a Future Circular Collider

R. BELUSEVIC

High Energy Accelerator Research Organization (KEK)
1-1 *Oho, Tsukuba, Ibaraki* 305-0801, *Japan*
belusev@post.kek.jp

Contents

Abstract :   This is the second paper by the author describing versatile accelerator complexes that could be built at a Future Circular Collider (FCC) in order to produce e^+e^-, $\gamma\gamma$ and ep collisions. The facility described here features an ILC-based e^+e^- collider placed tangentially to the FCC tunnel. If the collider is positioned asymmetrically with respect to the FCC tunnel, electron (or positron) bunches could be accelerated by both linacs before they are brought into collision with the 50-TeV beams from the FCC proton storage ring (FCC-pp). The two linacs may also form a part of the injector chain for FCC-pp. The facility could be converted into a $\gamma\gamma$ collider or a source of multi-MW beams for fixed-target experiments.

1   Introduction

The maximum luminosity at a circular e^+e^- collider, such as the proposed FCC-ee facility [1], is severely constrained by beamstrahlung effects at high energies; also, it is very difficult to achieve a high degree of beam polarization [2]. At the e^+e^- facilities described in this paper and [3], luminosity grows almost linearly with the beam energy [4] and the initial electron beam polarization can reach about 80% [5]. The availability of polarized beams is essential for some important precision measurements in e^+e^- and $\gamma\gamma$ collisions [6].

The rich set of final states in e^+e^- and $\gamma\gamma$ collisions would play an essential role in measuring the mass, spin, parity, two-photon width and trilinear self-coupling of the *Standard Model* (SM) Higgs boson, as well as its couplings to fermions and gauge bosons. Some of those measurements require centre-of-mass (c.m.) energies $\sqrt{s_{ee}}$ considerably exceeding those attainable at circular e^+e^- colliders. For instance, one has to measure separately the HWW, HHH and Htt couplings at $\sqrt{s_{ee}} \gtrsim 500$ GeV in order to determine the corresponding SM loop contributions to the effective HZZ coupling [7]. This would not be possible to accomplish using the proposed FCC-ee facility.

The Htt coupling cannot be *directly measured* in e^+e^- interactions below $\sqrt{s_{ee}} \approx 500$ GeV, since the cross-section for the relevant process is negligible (see Fig. 1). The HHH coupling can be *directly measured* at energies above the kinematic threshold for $e^+e^- \to$ ZHH, or by using the WW-fusion channel at $\sqrt{s_{ee}} \gtrsim 1$ TeV. *Indirect* and *model dependent* measurements of the HHH coupling are possible at lower energies by exploiting the loop corrections to single Higgs channels. However, the sensitivity of such measurements is very low, as can be inferred from Fig. 4 in [8].

Since the Higgs-boson mass affects the values of electroweak observables through radiative corrections, high-precision electroweak measurements provide a natural complement to direct studies of the Higgs sector. All the measurements made at LEP and SLC could be repeated at the facility described in this note, but at much higher luminosities and using 80% polarized electron beams [9]. The importance of beam polarization for some high-precision measurements was already stressed.

If electron or positron bunches are brought into collision with the 50-TeV proton beams from the FCC-pp storage ring, one would obtain an important source of deep-inelastic ep interactions.[1] Such interactions would yield valuable information on the quark-gluon content of the proton, which is crucial for precision measurements at the FCC-pp. The physics potential of a TeV-scale ep collider is comprehensively discussed in [11].

---

[1]The proposed FCC-eh electron-proton collider [10] would provide a higher luminosity than the facilities described in this paper and [3], but would have a considerably lower electron beam energy (around 60 GeV).
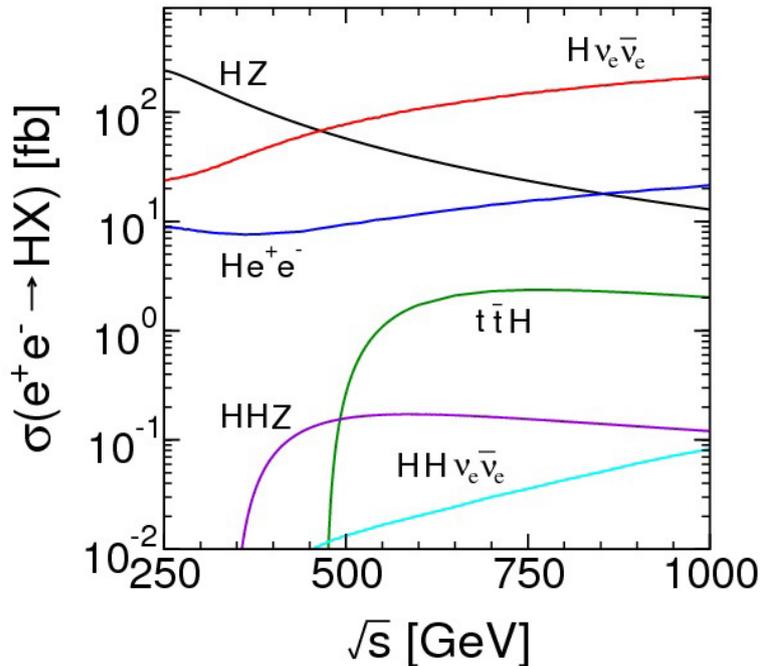
Figure 1: Centre-of-mass energy dependence of various cross-sections for single and double SM Higgs-boson production in e^+e^- annihilations [12].

A two-linac collider or an SLC-type facility [3] could be constructed in several stages, each with distinct physics objectives that require particular centre-of-mass energies (see Fig. 1):

- $e^+e^- \to Z$, WW; $\quad \gamma\gamma \to H$ $\qquad\qquad \sqrt{s_{ee}} \sim 90$ to 180 GeV

- $e^+e^- \to HZ$ $\qquad\qquad\qquad\qquad\qquad \sqrt{s_{ee}} \sim 250$ GeV

- $e^+e^- \to t\bar{t}$; $\quad \gamma\gamma \to HH$ $\qquad\qquad \sqrt{s_{ee}} \sim 350$ GeV

- $e^+e^- \to HHZ$, $Ht\bar{t}$, $H\nu\bar{\nu}$ $\qquad\qquad \sqrt{s_{ee}} \gtrsim 500$ GeV

For some processes within and beyond the SM, the required c.m. energy is considerably lower in $\gamma\gamma$ collisions than in e^+e^- or proton-proton interactions. For example, the heavy neutral MSSM Higgs bosons can be created in e^+e^- annihilations only by associated production ($e^+e^- \to H^0 A^0$), whereas in $\gamma\gamma$ collisions they are produced as single resonances ($\gamma\gamma \to H^0$, A^0) with masses up to 80% of the initial e^-e^- collider energy [3].

2 An ILC-based $e^+e^-/\gamma\gamma/ep$ facility at FCC

The ILC-based facility at a Future Circular Collider (FCC) shown in Fig. 2 features a superconducting two-linac e^+e^- collider placed tangentially to the FCC tunnel. Using an optical free-electron laser, the linacs could be converted into a high-luminosity $\gamma\gamma$ collider.

As mentioned in the Introduction, the maximum luminosity at a circular e^+e^- collider is severely constrained by beamstrahlung effects at high energies; also, it is very difficult to achieve a high degree of beam polarization. At the e^+e^- facilities described in this paper and [3], luminosity grows almost linearly with the beam energy and the electron beam polarization can reach 80%.

Table 1: Baseline ILC parameters [13]

Centre-of-mass energy	$\sqrt{s_{ee}}$	GeV	250	500
Pulse repetition rate	$f_{\rm rep}$	Hz	5	5
Bunch population	N_e	$\times 10^{10}$	2	2
Number of bunches	$N_{b,e}$		1312	1312
Bunch interval	$\Delta t_{b,e}$	ns	554	554
RMS bunch length	$\sigma_{z,e}$	mm	0.3	0.3
Norm. horizontal emittance at IP	ε_x^n	μm	10	10
Norm. vertical emittance at IP	ε_y^n	nm	35	35
Horizontal beta function at IP	β_x^*	mm	13	11
Vertical beta function at IP	β_y^*	mm	0.41	0.48
RMS horizontal beam size at IP	σ_x^*	nm	729	474
RMS vertical beam size at IP	σ_y^*	nm	7.7	5.9
Vertical disruption parameter	D_e		24.5	24.6
Luminosity	$\mathcal{L}_{ee}$	$\times 10^{34}\ cm^{-2}\,s^{-1}$	0.75	1.8

The baseline parameters for the proposed ILC collider, shown in Table 1, reflect the need to balance the constraints imposed by the various accelerator sub-systems, as explained in [13]. The rf power is provided by 10 MW multi-beam klystrons, each driven by a 120 kV pulse modulator. The estimated AC power is 122 MW at $\sqrt{s_{ee}} = 250$ GeV and 163 MW at $\sqrt{s_{ee}} = 500$ GeV. The 1.3-GHz superconducting niobium rf cavities have average accelerating gradients of 31.5 MeV/m.

In order to maximize luminosity at low centre-of-mass energies, the beam power could be increased by increasing the pulse repetition rate $f_{\rm rep}$ while reducing the accelerating gradient of the main linacs. At $\sqrt{s_{ee}} = 250$ GeV, the power consumption of the main 250-GeV linacs is reduced by over a factor of two when they are running at half their nominal gradient. Under these conditions, one can run the accelerator at the maximum repetition rate of 10 Hz (determined by the cryogenic system and the beam damping time $t_{\rm damp} \approx 80$ ms), thus doubling its luminosity.

The two superconducting L-band linacs in Fig. 2 may also form a part of the FCC-pp injector chain. Since the collider is positioned asymmetrically with respect to the FCC tunnel, electron (or positron) bunches could be accelerated by both linacs before they are brought into collision with the 50-TeV beams from the FCC-pp proton storage ring. The entire accelerator complex would serve as a source of e^+e^-, $\gamma\gamma$, pp and ep interactions.

3   Main parameters of a linac-ring ep collider at FCC

The idea to combine a 140-GeV electron linac and a 20-TeV proton storage ring in order to produce ep interactions at very high c.m. energies was put forward in 1979 as a possible option at the SSC proton collider [14]. In 1987 it was proposed to place a 2-TeV linear e^+e^- collider (VLEPP) tangentially to a 6-TeV proton-proton collider (UNK) at IHEP in Protvino [15], with the aim of obtaining both ep and γp collisions. Similar proposals for lepton-hadron and photon-hadron colliders at HERA, LHC and FCC have since been made (see [16] and references therein).
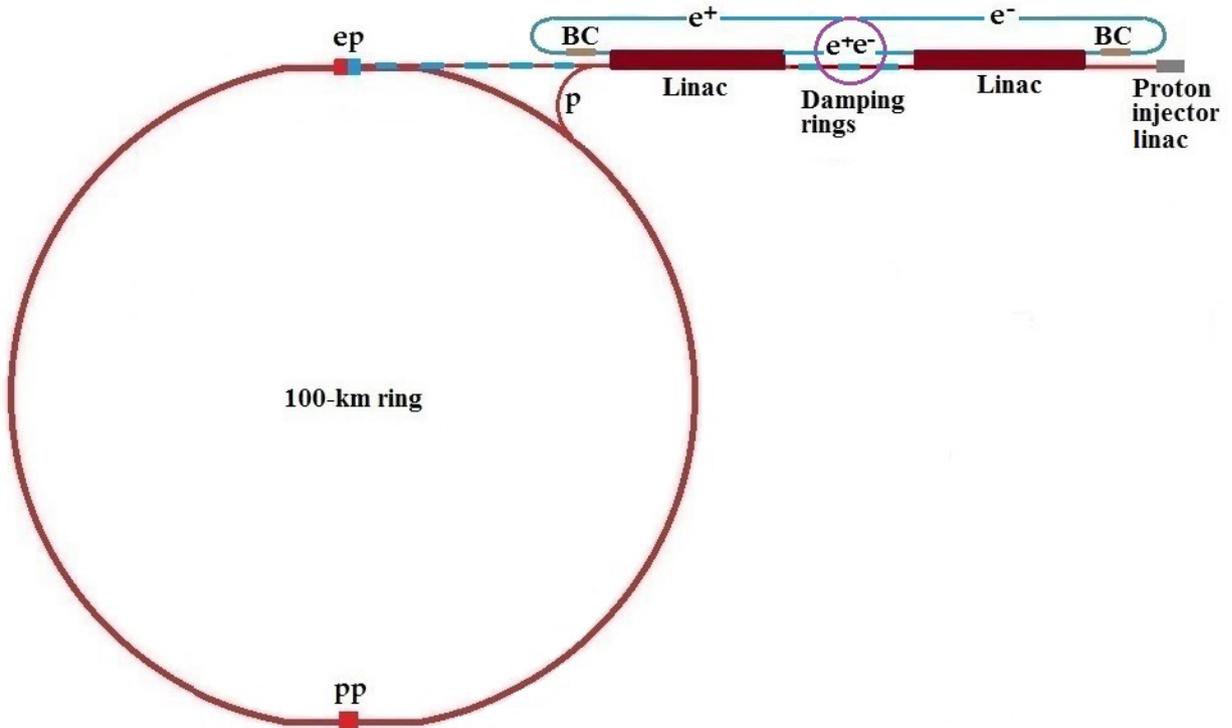
Figure 2: An ILC-based facility at FCC (BC stands for *bunch compression*). Electron (or positron) bunches are accelerated by both linacs before their collision with the 50-TeV proton beam from the FCC-pp storage ring. The two superconducting L-band linacs may form the low-energy part of the FCC-pp injector chain. A much cheaper alternative to this facility is described in [3].

The facility shown in Fig. 2 is an ILC-based version of the original VLEPP⊗UNK design. Since the collider is positioned asymmetrically with respect to the FCC tunnel, electron (or positron) bunches could be accelerated by both linacs (which contain *standing wave cavities*) before they are brought into collision with the 50-TeV beams from the FCC-pp proton storage ring.

An ILC-type linac is a suitable source of electron beams for an electron-proton collider, because: (1) the spacing between electron bunches can be made to match that between the proton bunches in the FCC-pp storage ring, and (2) the length of an electron 'bunch train' corresponds roughly to the FCC ring circumference. This is not the case, for instance, with an X-band linac, where the electron bunch spacing (~ 1 ns) is much shorter than that between proton bunches at the FCC-pp (see Table 2).

In *head-on collisions* of ultra-relativistic electrons and protons, the centre-of-mass energy is $\sqrt{s_{ep}} = 2\sqrt{\mathrm{E}_e \mathrm{E}_p}$. The total electron beam current $I_e = \mathcal{P}_e/\mathrm{E}_e$ is limited by the maximum allowed beam power $\mathcal{P}_e$ for a given electron beam energy E_e. Assuming that round electron and proton beams of equal transverse sizes are colliding head-on at the interaction point (IP),[2] the luminosity of the collider is given by [17][18]

$$\mathcal{L}_{ep} = f_c \frac{N_e N_p}{4\pi\sigma_p^2}\, \mathcal{H} \equiv \frac{I_e}{4\pi\mathrm{e}}\frac{N_p}{\varepsilon_p^n}\frac{\gamma_p}{\beta_p^*}\, \mathcal{H} \tag{1}$$

In these expressions, N_e and N_p are the electron and proton bunch populations, respectively; f_c is the bunch collision frequency; $\mathcal{H}$ is a correction factor discussed below; and $\sigma_p = \sqrt{\varepsilon_p^n \beta_p^*/\gamma_p}$ is the proton beam size at IP, expressed in terms of the normalized proton beam emitance, ε_p^n, the proton beta function at IP, β_p^*, and the Lorentz factor of the proton beam, γ_p. Note that the

---

[2]The two beams are chosen to have roughly equal transverse sizes in order to reduce adverse effects a much smaller electron beam could have on the proton beam lifetime. Electron bunches are discarded after each collision.

Table 2: Baseline FCC-pp parameters [19][20]. Numbers inside round brackets represent parameters for 5 ns bunch spacing.

Beam energy	E_p	TeV	50
Initial bunch population	N_p	$\times 10^{10}$	10 (2)
Number of bunches	$N_{b,p}$		10600 (53000)
Bunch interval	$\Delta t_{b,p}$	ns	25 (5)
RMS bunch length	$\sigma_{z,p}$	mm	80
Norm. transverse emittance	ε_p^n	μm	2.2 (0.44)
Beta function at IP	β_p^*	m	0.3
Beam size at IP	σ_p	μm	6.8 (3)
Beam-beam tune shift/IP	ΔQ_p		0.005
Luminosity/IP	$\mathcal{L}_{ep}$	$\times 10^{32}\ cm^{-2}\ s^{-1}$	2.3

luminosity is proportional to the electron beam power $\mathcal{P}_e = eN_e f_c E_e = I_e E_e$ (e is the electron charge), the proton beam energy (γ_p), and the proton beam brightness N_p/ε_p^n.

In Eq. (1), $\mathcal{H}$ is a product of three correction factors with values typically close to unity:

$$\mathcal{H} \equiv H_{\text{hourglass}} \cdot H_{\text{pinch}} \cdot H_{\text{filling}} \tag{2}$$

The factor H_{filling} takes into account the filling patterns of the electron and proton beams. If the number of proton bunches $N_{b,p} = 10600$ and the bunch interval $\Delta t_{b,p} = 25$ ns (see Table 2), the 'length' of the proton beam is 2.65×10^5 ns. This corresponds to 80 km, which means that only 80% of the FCC circumference is filled with proton bunches ($H_{\text{filling}} = 0.8$). In this particular case 20% of the electron bunches would not collide with the proton beam.

The factor $H_{\text{hourglass}}$ accounts for a loss of luminosity when the bunch length is comparable to or larger than β^*. The beta function $\beta(s) = \beta^* + s^2/\beta^*$ grows parabolically as a function of distance s from the interaction point, which causes the beam size to increase:

$$\sigma(s) = \sqrt{\beta(s) \cdot \varepsilon} \approx s\sqrt{\varepsilon/\beta^*} \tag{3}$$

As the beam size increases, the contribution to the luminosity from regions with large σ decreases (*hourglass effect*). For zero crossing angle and $\sigma_{z,p} \gg \sigma_{z,e}$,

$$H_{\text{hourglass}}(x) = \sqrt{\pi}\, x\, e^{x^2}\, \text{erfc}(x) \tag{4}$$

with

$$x \equiv \frac{2\beta_e^*}{\sigma_{z,p}} \frac{\varepsilon_e/\varepsilon_p}{\sqrt{1 + (\varepsilon_e/\varepsilon_p)^2}}, \qquad \text{erfc}(x) = \frac{2}{\sqrt{\pi}} \int_x^\infty e^{-t^2}\, dt \tag{5}$$

where ε_e and ε_p denote *geometric emittances* [11][21] (the normalized emittance $\varepsilon^n = \gamma\varepsilon$ is invariant under acceleration); erfc(z) is the 'complementary error function' (defined as the area under the 'tails' of a Gaussian distribution).

The enhancement factor H_{pinch} in Eq. (2) is due to the attractive *beam-beam force*. Since the electron bunch charge is relatively small and the proton energy is high, the beam-beam force acting on electrons has a much greater strength than that acting on protons. Consequently, the electron bunch is focused by the protons during a collision,. This leads to a reduction in the transverse
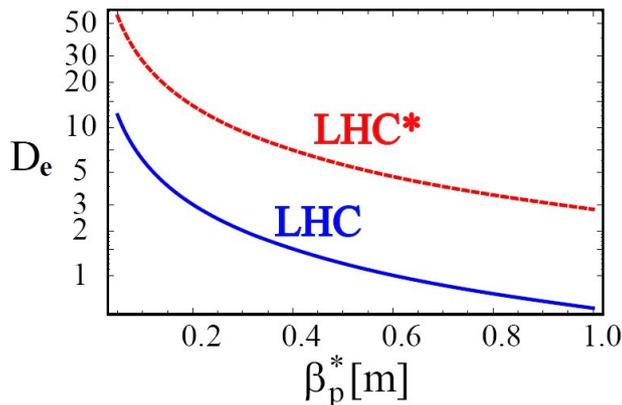
Figure 3: Electron beam disruption parameter D_e as a function of β_p^* [18]. The plot was made for an *ep* collider based on LHC and an ILC-type electron linac. LHC* denotes an upgraded proton beam scenario (see Table 1 in [18]).

electron beam size ('pinch effect') and hence to an increase in the luminosity. The effect can be simulated using the program *Guinea-Pig* (see [10] and references therein, as well as Table 3 below).

One can ignore the longitudinal structure of electron bunches because they are much shorter than proton bunches. In this case the *transverse disruption* of the electron beam during a collision is described by the parameter [22][23]

$$D_e = \frac{r_e}{\gamma_e} \frac{N_p \sigma_{z,p}}{\sigma_p^2} \tag{6}$$

where γ_e is the Lorentz factor of the electron beam, $r_e \approx 2.82 \times 10^{-15}$ m is the classical radius of the electron, and $\sigma_{z,p}$ is the proton bunch length. For $\beta_p^* = 10$ cm, the disruption parameter can be as large as $D_e \approx 20$ in an *ep* linac-ring collider (see Fig. 3).

As already mentioned, the luminosity of an *ep* collider is proportional to the proton *beam brightenss* N_p/ε_p^N (see Eq. (1)). Together with a given bunch length and energy spread, the beam brightness is a measure of the phase-space density. In the low-energy part of a proton injector, the quantity N_p/ε_p^n is limited by space-charge forces that induce a *transverse tune shift*[3]

$$\Delta Q_{sc} \propto \frac{N_p}{\varepsilon_p^n} \frac{1}{(v_p/c)^2 \gamma_p^2} \tag{7}$$

Here v_p is the proton velocity and c is the speed of light in vacuo [24][25]. In order to reduce the effect of space-charge forces at low energies and deliver proton bunches a few mm long, the facility in Fig. 2 features a single 3-GeV proton injector linac similar to that currently being built at the *European Spallation Source* (ESS) [26].

At high energies, the beam brightness in a storage ring slowly diminishes due to Coulomb scattering of protons within a bunch (*intra-beam scattering*) [27]. In the presence of *dispersion* (see footnote 4), the intra-beam scattering also leads to an increase in emittance. This sets the ultimate limit on the phase-space density in a proton storage ring. The growth of a beam of charged particles due to intra-beam scattering is characterized by the horizontal *growth rate* [28]

$$\tau_x^{-1} \propto \frac{N_p}{\varepsilon_x^n \varepsilon_y^n \varepsilon_l^n} \tag{8}$$

---

[3]The 'tune' or Q value is defined as the number of betatron oscillations per revolution in a circular accelerator. The charge and current of a high-inensity beam in an accelerator create self-fields and image fields that alter the beam dynamics and influence the single-particle motion as well as coherent oscillations of the beam as a whole. The effect of space-charge forces is to change Q by an amount ΔQ_{sc} ('tune shift') [24].

where $\varepsilon_{x,y}^n$ are the normalized beam emittances, $\varepsilon_l^n \equiv \beta\gamma\sigma_{z,p}\sigma_{\Delta p/p}$ and $\sigma_{\Delta p/p}$ is the r.m.s. relative momentum $\Delta p/p$. Note that the growth rate depends linearly on the normalized phase-space density. In the FCC-pp storage ring synchrotron radiation damping is expected to be much stronger than the intra-beam scattering, making the latter effect less of an issue [19].

The space-charge forces that limit the beam brightness are determined by the longitudinal charge density and thus by the proton bunch length $\sigma_{z,p}$. To attain maximum brightness, $\sigma_{z,p}$ should be as large as possible. On the other hand, there is a loss of luminosity when the bunch length is comparable to or larger than β^* (this *hourglass effect* was described earlier). Furthermore, the transverse disruption of the electron beam during an *ep* collision is proportional to $\sigma_{z,p}$, as shown in Eq. 6. While optimizing the bunch length within these constraints, the beam stability must be preserved (see below).

A particle in one colliding beam experiences a force due to the electromagnetic interactions with all the particles in the opposing beam. This force depends upon the displacement of the particle from the equilibrium orbit of the opposing bunch. For small particle displacements, the beam-beam interaction is nearly linear, and its strength is characterized by a parameter known as the *beam-beam tune shift* [29]:

$$\Delta Q_p \equiv \frac{r_p}{4\pi}\frac{N_e}{\sigma_e^2}\frac{\beta_p^*}{\gamma_p} \approx \frac{r_p N_e}{4\pi\varepsilon_p^n} \tag{9}$$

where $r_p \approx 1.53 \times 10^{-18}$ m is the classical radius of the proton and $\sigma_p \approx \sigma_e$ was used. Since electron bunches are discarded after each collision, only the tune shift of the proton beam, ΔQ_p, is considered here. The tune shift is approximately given by

$$\Delta Q_p \approx 1.2 \times 10^{-3} \cdot \frac{N_e[10^{10}]}{\varepsilon_p^n[10^{-6}\,m]} \tag{10}$$

The parameter ΔQ_p must be limited to about 4×10^{-3} in order to stem the emittance growth due to random fluctuations of the electron bunch parameters [30]. This imposes an upper limit of $N_e \lesssim 3 \times 10^{10}$ if one assumes $\varepsilon_p^n \approx 10^{-6}$ m (see also Table 4 in [31]).

A small error Δk in the quadrupole gradient leads to a tune shift ΔQ_k. To a beam particle with momentum $p = p_0 + \Delta p$ it appears that all the quadrupoles in the ring have a quadrupole error proportional to $\Delta p/p_0$ [32]. The dimensionless quantity ξ defined by $\Delta Q_k \equiv \xi(\Delta p/p_0)$ is called the *chromaticity* of the beam optics. This quantity increases with the strength of the beam focusing. The main contribution to the chromaticity comes from the final focus quadrupoles, where the β-function is large [33]:

$$\xi \approx \beta_q k_q \ell_q \approx \frac{\ell^* + \ell_q/2}{\beta_y^*} \tag{11}$$

Here β_q, k_q and ℓ_q denote the beta function, field gradient and length of the final quadrupole, respectively; ℓ^* is the focal length and β_y^* the value of the vertical β-function at the interaction point. Thus, the chromaticity increases as β_y^* decreases.

Since ξ grows linearly with the distance between the final-focus quadrupole and the interaction point, it is desirable to make this distance as small as possible. For the interaction region at an electron-proton collider, a novel design technique called the *achromatic telescopic squeezing* (ATS) has been proposed "in order to find the optimal solution that would produce the highest luminosity while controlling the chromaticity, minimizing the synchrotron radiation power and maintaining the dynamic aperture required for [beam] stability" [34][35] (*dynamic aperture* is the stability region of phase space in a circular accelerator).

The issue of beam stability was addressed earlier concerning the optimization of the proton bunch length. The proton bunches inside an ILC-type linac are much shorter than those inside the FCC storage ring (the 3-GeV injector linac mentioned earlier would deliver bunches a few

Table 3: Parameters of the proposed linac-ring *ep* collider.

Electron beam parameters			
Beam energy	E_e	GeV	500
Initial bunch population	N_e	$\times 10^{10}$	2
Number of bunches	$N_{b,e}$		3200
Bunch interval	$\Delta t_{b,e}$	ns	211.376
RF frequency	f_{RF}	MHz	1301
Pulse repetition rate	f_{rep}	Hz	5
Duty cycle	d	%	0.34
Beam power	$\mathcal{P}_e$	MW	25.5
Proton beam parameters			
Beam energy	E_p	TeV	50
Initial bunch population	N_p	$\times 10^{10}$	10
Number of bunches	$N_{b,p}$		5300
RMS bunch length	$\sigma_{z,p}$	mm	80
Bunch interval	$\Delta t_{b,p}$	ns	49.7355
RF frequency	f_{RF}	MHz	401.968
Collider parameters			
Beta function at IP	β_p^*	m	0.1
Norm. transverse emittance	ε_p^n	μm	1
Beam-beam tune shift	ΔQ_p		0.0024
Electron beam disruption	D_e		11.3
Hourglass factor	$H_{\mathrm{hourglass}}$		0.81
Pinch factor	H_{pinch}		1.3
Proton filling	H_{filling}		0.79
Luminosity	$\mathcal{L}_{ep}$	$\times 10^{32}\ cm^{-2}\,s^{-1}$	1.08

millimetres long). Thus, $\sigma_{z,p}$ has to be increased in order to attain the baseline FCC-pp value (see Table 2). In principle, the easiest way to increase the bunch length in a circular accelerator is to switch all RF systems off and let the bunches 'decay' due to *dispersion*.[4] A faster and more subtle method — which could be implemented using a 3-TeV proton booster placed inside the FCC tunnel — is described in [36].

The expressions for beam-beam tune shift, electron beam disruption and beam growth rate given above do not accurately describe the *time-dependent beam dynamics* during collisions. To study the time-dependent effects caused by varying beam sizes, collision point simulations for linac-

---

[4]A particle with a momentum difference $\Delta p/p$ has a transverse position $x(s) + D(s)\Delta p/p$, where $x(s)$ is the position a particle of nominal momentum would have and $D(s)$ is the *dispersion function*.

ring ep colliders have been performed using the ALOHEP software [37]. This numerical program optimizes a set of electron and proton beam parameters in order to maximize luminosity [38].

The luminosity $\mathcal{L}_{ep}$ is independent of the electron bunch charge and the collision frequency as long as their product, expressed in terms of the beam power $\mathcal{P}_e$, is constant. One can therefore rewrite Eq. (1) as follows [17][39]

$$\mathcal{L}_{ep} = 4.8 \times 10^{30}\,\mathrm{cm^{-2}\,s^{-1}} \cdot \frac{N_p}{10^{11}} \frac{10^{-6}\,\mathrm{m}}{\varepsilon_p^n} \frac{\gamma_p}{1066} \frac{10\,\mathrm{cm}}{\beta_p^*} \frac{\mathcal{P}_e}{22.6\,\mathrm{MW}} \frac{250\,\mathrm{GeV}}{\mathrm{E}_e} \cdot \mathcal{H} \qquad (12)$$

The electron beam current $I_e = \mathrm{e}N_e f_{b,e} = 15$ mA, where $f_{b,e}$ is the inverse of the bunch interval (see Table 3). The electron beam power $\mathcal{P}_e = \mathrm{E}_e I_e d = 25.5$ MW, where d is the linac duty cycle. The proton beam current $I_p = 320$ mA, and the total energy stored per proton beam is 4.2 GJ. To calculate $H_{\mathrm{hourglass}}$, we set $\beta_e^* \approx \beta_p^*$ [35]. The value of H_{pinch} was taken from [10].

4 Acknowledgements

References

[1] A. Blondel and F. Zimmermann, CERN-OPEN-2011-047; arXiv:1112.2518 (2012).

[2] M. Koratzinos, arXiv:1511.01021v1 (2015).

[3] R. Belusevic, J. Mod. Phys. **8**, pp 1–16 (2017).

[4] M. Boscolo, J.-P. Delahaye and M. Palmer, arXiv:1808.01858 (2018).

[5] B. Aurand et al., Proc. Intl. Linear Collider Workshop (LCWS08 and ILC08), Chicago, Illinois, 2008; arXiv:0903.2959 (2009).

[6] G. Moortgat-Pick et al., Eur. Phys. J. C **75**: 371 (2015).

[7] M. McCullough, arXiv:1312.3322v6 (2014).

[8] S. Di Vita et al., DESY 17-131, FERMILAB-PUB-17-462-T and arXiv:1711.03978 (2017).

[9] J. Erler et al., Phys. Lett. B **486**, 125 (2000).

[10] O. Bruning et al., CERN-ACC-2017-0019 (2017).

[11] J. L. Abelleira Fernandez, J. Phys. G: Nucl. Part. Phys. **39**, 075001 (2012).

[12] D. Asner et al., arXiv:1310.0763v3 (2013).

[13] C. Adolphsen et al., *The International Linear Collider Technical Design Report*, Volume 3.II; arXiv:1306.6328.

[14] G. Weber et al., Proc. 2nd ICFA Workshop on Possibilities and Limitations of Accelerators and Detectors, Les Diablerets, Switzerland, 4–10 Oct. 1979, pp 199–221.

[15] S. I. Alekhin et al., IHEP Preprint 87–48, Serpukhov (1987).

[16] A. N. Akay, H. Karadeniz and S. Sultansoy, Int. J. Mod. Phys. A **25**, No. 4, pp 4589–4602 (2010).

[17] M. Tigner, B. Wiik and F. Willeke, Proc. 1991 IEEE Part. Accel. Conf., San Francisco, California (1991).

[18] F. Zimmermann et al., Proc. EPAC2008, Genoa, Italy, pp 2847–2849 (2008).

[19] M. Benedikt, D. Schulte and F. Zimmermann, Phys. Rev. Spec. Topics — Accel. Beams **18**, 101002 (2015).

[20] F. Zimmermann, Nucl. Instrum. Meth. B **355**, pp 4–10 (2015).

[21] M. A. Furman, Proc. 1991 IEEE Particle Accelerator Conference, San Francisco, California, pp 422–424 (1991).

[22] K. Yokoya and P. Chen, *Beam-beam phenomena in linear colliders*, Lectures at the US-CERN School on Particle Accelerators, Hilton Head Island, South Carolina, USA, 1990; printed in Lecture Notes in Physics 400, Springer-Verlag, pp 415-445 (1992).

[23] Y. Hao and V. Ptitsyn, Phys. Rev. Spec. Topics — Accel. Beams **13**, 071003 (2010).

[24] K. Schindl, *Space charge*, Proc. Joint US-CERN-Japan-Russia School on Particle Accelerators, Beam Measurements, Montreux, 1998, edited by S. Kurokawa, S.Y. Lee, E. Perevedentsev, S. Turner, World Scientific, pp 127–151 (1999).

[25] M. Benedikt and R. Garoby, CERN-AB-2005-009.

[26] H. Danared, M. Lindroos and C. Theroine, ESS: *neutron beams at the high-intensity frontier*, CERN Courier, June 2014, pp 21–24.

[27] A. Piwinski, in *Proc. 9th Int. Conf. on High Energy Accelerators, Stanford* (1975).

[28] G. Parzen, Nucl. Instr. Meth. **A 256**, pp 231–240 (1987).

[29] F. Ruggiero and F. Zimmermann, Phys. Rev. Spec. Topics — Accel. Beams **5**, 061001 (2002).

[30] R. Brinkmann, Turk. J. Phys. **22**, pp 661-666 (1998).

[31] Ö. Yavas, Turk. J. Phys. **22**, pp 667-673 (1998).

[32] K. Wille, *The Physics of Particle Accelerators*, Oxford Univ. Press, 2000.

[33] F. Zimmermann, *Accelerator Physics and Technologis for Linear Colliders*, Physics 575 lecture notes, University of Chicago (2002).

[34] S. Fartoukh, *Achromatic telescopic squeezing scheme and application to the* LHC *and its luminosity upgrade*, Phys. Rev. Spec. Topics — Accel. Beams **16**, 111002 (2013).

[35] E. Cruz-Alaniz et al., Phys. Rev. Spec. Topics — Accel. Beams **18**, 111001 (2015).

[36] H. Damerau, Ph.D. Thesis, Technical Univ. Darmstadt, 2005.

[37] ALOHEP, https://alohep.hepforge.org; hosted by HepForge, IPPP Durham University.

[38] Y. C. Acar et al., Nucl. Instr. Meth. **A 871**, pp 47–53 (2017).

[39] The THERA Book, edited by U. Katz, M. Klein, A. Levy and S. Schlenstedt, DESY 01-123F, Vol. 4, DESY-LC-REV-2001-062 (2001).